Journal of
Ceramic Science
and Technology

J. Ceram. Sci. Tech., 07 [01] 47-52 (2016)
DOI: 10.4416/JCST2015-00027
available online at: http://www.ceramic-science.com

First-Principles Study of a New Higher-Order MAX Phase of $Ti_5Al_2C_3$

X.-K. Qian[1, 2, 3], H.-Y. Wu*[3], H.-P. Zhu[4], S.-H. Ma[3], T. Jiang[2]

[1]School of Materials Science and Engineering, Zhejiang University, Hangzhou 310027, PR China
[2]Zhejiang Super Lighting Electric Appliance Limited Company, Lishui 321403, PR China
[3]School of Engineering and Design, Lishui University, Lishui 323000, PR China
[4]School of Ecology, Lishui University, Lishui 323000, PR China

received June 15, 2015; received in revised form July 23, 2015; accepted August 23, 2015

Abstract

The crystal structure of a new phase plays an important role in understanding its properties. The structure, elastic and electronic properties of $Ti_5Al_2C_3$ are studied based on first-principles calculations. The simulated lattice parameter and internal coordinates are found to be in good agreement with the experimental values. It is shown that this new phase is mechanically stable. The elastic properties are estimated from the individual elastic constants with the help of Hill's approximation. The bulk modulus, shear modulus, Young's modulus, Poisson's ratio, theoretical density and Debye temperature of $Ti_5Al_2C_3$ are calculated to be 147 GPa, 124 GPa, 290 GPa, 0.17, 4.12 g/cm^3 and 759 K, respectively. The band structure and DOS reveal that $Ti_5Al_2C_3$ is conductive. At the Fermi level (E_f), the energy band is contributed mainly by the Ti 3d state and secondarily by the Al 3p state. Ti-Al hybridizations are located just below the E_f and are weaker than the Ti-C bonds, which are much deeper in energy.

Keywords: $Ti_5Al_2C_3$, first-principles, mechanical stability, electronic structure

I. Introduction

The ternary-layered carbides and nitrides of the $M_{n+1}AX_n$ phases (abbreviated as MAX phases), where n = 1, 2, or 3, M being of a transition metal, A being of a group A element mostly from groups of IIIA or IVA, and X being of C or N, have been extensively studied in recent years on account of their unique properties [1–4]. Similar to metals, the MAX phases are excellent electric and thermal conductors with exceptional thermal shock resistance and damage tolerance [5–10]. They also exhibit resistance to oxidation [11–14] and corrosion [15–16]. Furthermore, they are quite elastic, yet readily machinable [17–18]. These salient properties make them suitable for various potential applications in which radiation damage tolerance [19], resistance to ultra-high-temperature ablation [20], self-lubrication [21–22] and so on are required. According to the value of *n*, the MAX phases can be further categorized as 211 (*n* = 1), 312 (*n* = 2), and 413(*n* = 3) types [1]. Up to now, over sixty members have been identified.

The 523 phase is a new-type member of the MAX phases, which cannot be described with the conventional $M_{n+1}AX_n$formula. The 523 phase carbides including $Ti_5Si_2C_3$ [23], $Ti_5Ge_2C_3$ [24], $Ti_5Al_2C_3$ [25], and $(V,Cr)_5Al_2C_3$ [26] together with the conventional MAX phases follow another general formula $M_nA_mX_{n-m}$ ($n \geq 2m$, *n* and *m* are integers) [27]. These new members belong to another category that is called higher-order MAX phases. A review of the higher-order MAX phases can be found elsewhere [2, 28]. To date, higher-order phases have been observed mostly in thin films. $Ti_5Si_2C_3$ was first reported in the Ti-Si-C film by Palmquist *et al.* [23].

$Ti_5Al_2C_3$ was reported to grow interiorly in bulk Ti_2AlC by Lin *et al.* [29] and was found in Ti_2AlC thin films by Wilhelmsson *et al.* [30]. In both cases, however, the $Ti_5Al_2C_3$ was only observed with TEM to exist in small domains. Consequently, the XRD pattern could not be collected. Recently, bulk $Ti_5Al_2C_3$ was synthesized based on the topotactic transformation of Ti_2AlC under Ar after 8 h at 1500 °C[25] by Lane *et al.* and by means of reactive hot pressing of a mixture of Ti, Al and graphite powders with a nominal molar ratio of Ti:Al:C = 5:2.15:2.78 at 1580 °C for 1 h by Wang *et al.* [31]. Wang *et al.* [31] claimed that $Ti_5Al_2C_3$ crystallizes in hexagonal structure with *P*63/*mmc* space group symmetry. The crystal structure has Ti1 and Ti2 at Wyckoff position 4f, Ti3 at 2d, Al at 4e, C1 at 2a, and C2 at 4e with lattice parameters of *a* = 3.038 Å and *c* = 32.261 Å. However, different opinions on the crystal structure of this new compound are presented [32]. Lane *et al.* deduced that the stacking sequence of $Ti_5Al_2C_3$ can be considered as the alternate layers of Ti_2AlC and Ti_3AlC_2. It was concluded that $Ti_5Al_2C_3$ crystallizes in a trigonal structure with *P*3*m*1 space group. The crystal structure consists of three formula units and the lattice parameter is *a* = 3.064 Å and *c* = 48.23 Å. Zhang *et al.* [27] analyzed the crystal structure of $Ti_5Al_2C_3$ with the combined techniques of XRD, convergent beam electron diffraction and *ab initio* calculations. They demonstrated that the $R\bar{3}m$ space group better fits the experimental XRD result. The lattice parameter is *a* = 3.0564 and *c* = 48.1846 Å in a hexagonal unit cell.

* Corresponding author: why160@126.com

Table 1: Calculated structure parameters of $Ti_5Al_2C_3$ at zero pressure.

Formula		$Ti_5Al_2C_3$		
Method		Rietveld refined [27]	*Ab initio* calculation [27]	First-principle [this work]
Lattice parameter (nm)		a = 0.30564 c = 4.81846	a = 0.30752 c = 4.85868	a = 0.30735 c = 4.86254
Atom position	Ti1 (3*a*)	(000)	(000)	(000)
	Ti2 (6*c*)	(2/3, 1/3, 0.0497)	(2/3, 1/3, 0.0487)	(2/3, 1/3, 0.0487)
	Ti3 (6*c*)	(2/3, 1/3, 0.1428)	(2/3, 1/3,0.1431)	(2/3, 1/3,0.1431)
	Al (6*c*)	(0, 0, 0.0960)	(0, 0, 0.0961)	(0, 0, 0.0961)
	C1 (3*b*)	(0, 0, 0.5)	(0, 0, 0.5)	(0, 0, 0.5)
	C2 (6*c*)	(1/3, 2/3, 0.0275)	(1/3, 2/3, 0.0267)	(1/3, 2/3, 0.0266)

The first-principles calculations based on density-functional theory (DFT) aim to find eigenfunctions and eigenvalues of the Hamiltonian in a parameter-free approximation [33]. They have been successfully applied to obtain atomic and molecular information. Recently, DFT has been extensively employed to study new members of the MAX phases [34–39]. Generally speaking, theoretically calculated results agree well with the available experimental data. To date, theoretical studies on the newly synthesized $Ti_5Al_2C_3$ are insufficient [31, 40]. To make matters worse, these previous results are incorrect because the atomic positions and space group have been mistakenly employed. It is necessary to further explore the crystal structure and properties of this new ternary carbide. In this paper, we present a detailed and systematically theoretical study on the structural, mechanical and electronic properties of $Ti_5Al_2C_3$ based on the first-principles calculations.

II. Computational Details

The internal atom coordinates and the lattice parameters of $Ti_5Al_2C_3$ were independently optimized and the ground-state electronic structures were calculated using the standard CASTEP code [41], which employs the plane-wave pseudopotential method based on density functional theory. The plane-wave energy cutoff and the Brillouin zone sampling were fixed at 450 eV and 10 × 10 × 2 Monkhorst-Pack [42] special k-point meshes, respectively. Interactions of electrons with ion cores were represented by the Vanderbilit-type ultrasoft pseudopotential [43]. The electronic exchange-correlation energy was estimated according to the generalized-gradient approximation of Perdew, Burke and Ernzerhof (GGA-PBE) [44]. The Broyden-Fletcher-Goldfarb-Shanno (BFGS) algorithm [45] was used to minimize the total energy and internal forces. The tolerances for geometry optimization were set as the difference in total energy being within 5×10^{-6} eV/atom, the maximum ionic Hellmann-Feynman force being within 0.01 eV/Å, the maximum stress being within 0.02 GPa and the maximum ionic displacement being within 5×10^{-4} Å. The criteria for convergence in optimizing atomic internal freedoms were selected as follows: difference on total energy within 1×10^{-6} eV/atom, ionic Hellmann-Feynman forces within 0.002 eV/Å and maximum ionic displacement within 1×10^{-6} Å.

III. Results and Discussion

(1) Crystal structure and cohesive energy

As the first step, the geometrical structure was optimized at zero pressure. The equilibrium structure of $Ti_5Al_2C_3$ was obtained after the atomic position and lattice parameter were relaxed independently. The present results, previously experimental and simulated results for $Ti_5Al_2C_3$ are shown in Table 1. It can be seen that our simulated results are in good agreement with the previous data. The deviation from the experimental values of a and c is 0.6 % and 4.4 %, respectively. Therefore, the GGA-PBE approach provides a reliable estimation of the equilibrium structure parameters.

The cohesive energy is a measure of the strength of the forces that bind atoms together in the solids, and is important for understanding structural stability. The cohesive energy $E_{coh}^{Ti_5Al_2C_3}$ per atom is defined as the total energy of the constituent atoms at an infinite separation with the subtraction of total energy of the compound,

$$E_{coh}^{Ti_5Al_2C_3} = (5E_{atom}^{Ti} + 2E_{atom}^{Al} + 3E_{atom}^{C} - E_{total}^{Ti_5Al_2C_3})/10 \quad (1)$$

where $E_{total}^{Ti_5Al_2C_3}$ refers to the calculated total energy of $Ti_5Al_2C_3$ at 0 K at equilibrium state, and E_{atom}^{Ti}, E_{atom}^{Al} and E_{atom}^{C} are the pseudo-atomic energies of the pure constituents Ti, Al and C, respectively. The calculated cohesive energies of $Ti_5Al_2C_3$ is 7.71 eV/atom, indicating that $Ti_5Al_2C_3$ is a stable phase.

(2) Mechanical properties and Debye temperature

In order to study the mechanical properties of $Ti_5Al_2C_3$, the second-order elastic constants C_{ij}, bulk modulus B, shear modulus G, Young's modulus E, and Poisson's ratio μ from the individual elastic constants by Hill's approximation [46] are further calculated. The obtained values are listed in Table 2, together with the theoretical values of Ti_3AlC_2 and Ti_2AlC for comparison. It can be seen that $Ti_5Al_2C_3$ has smaller values for C_{11} and C_{33} than those of the Ti_3AlC_2, indicating a lower resistance against the principal strain ε_{11} and ε_{33}. The C_{11} of $Ti_5Al_2C_3$ is 11 GPa larger than that of Ti_2AlC, but the C_{33} is 39 GPa smaller. The C_{44} of $Ti_5Al_2C_3$ is smaller than those of the Ti_2AlC and Ti_3AlC_2, thereby indicating lower resistances to basal and prismatic shear deformations. The

bulk modulus B of $Ti_5Al_2C_3$ is lower than that of Ti_2AlC and Ti_3AlC_2, indicating a lower resistance to the volume change. The shear modulus G of $Ti_5Al_2C_3$ is very close to that of Ti_2AlC, suggesting a similar resistance to the shape change as Ti_2AlC. Furthermore, the Poisson's ratio μ of $Ti_5Al_2C_3$ is very close to that of Ti_3AlC_2 and Ti_2AlC.

The elastic constants of a material are very important because they are related to various fundamental solid-state properties and can provide valuable information about the mechanical stability. A necessary condition for a material to be mechanically stable is that its elastic constants should satisfy the well-known Born stability criteria. For a trigonal system, the criteria should obey the following conditions:

$$C_{11}>|C_{12}|,\ (C_{11}+C_{12})C_{33}>2C_{13}^2,\quad (C_{11}-C_{12})C_{44}>2C_{14}^2 \tag{2}$$

According to the calculated elastic constants, it is obvious that these criteria are satisfied for $Ti_5Al_2C_3$, and hence it is mechanically stable at zero pressure.

In thermodynamics and solid state physics, the Debye temperature (θ_D) is an important parameter and can effectively estimate the phonon contribution to the specific heat at low temperature. There are various methods to obtain the value of θ_D. In the present study, the θ_D of $Ti_5Al_2C_3$ is calculated by means of the mean sound velocity (v_m) using the following equation [48]:

$$\theta_D=\frac{h}{k}\left(\frac{3n}{4\pi}\frac{N_A\rho}{M}\right)^{\frac{1}{3}}\nu_m \tag{3}$$

where h is the Plank's constant, k is Boltzmann's constant, n is the number of atoms in the molecule, π is the circumference ratio, N_A is Avogadro's number, ϱ is the density and M is the molecular weight. The mean sound velocity in the polycrystalline materials is estimated approximately with the following equation [49]:

$$\nu_m=\left[\frac{1}{3}\left(\frac{1}{\nu_l^3}+\frac{2}{\nu_t^3}\right)\right]^{-1/3} \tag{4}$$

where v_l and v_t are the longitudinal and transverse sound velocity, respectively. They are determined with the shear modulus (G) and the bulk modulus (B) from Navier's equation [49]:

$$\nu_l=\sqrt{(B+4G/3)/\rho}\ \text{and}\ \nu_t=\sqrt{G/\rho} \tag{5}$$

The theoretical density and θ_D of $Ti_5Al_2C_3$ are calculated to be 4.12 g/cm^3 and 759 K, respectively. Unfortunately, as far as we are aware, no experimental data are available for comparison with these simulated values.

(3) Electronic properties and bonding characteristics

To obtain an insight into the electronic properties of the $Ti_5Al_2C_3$, its band structure is further examined. The band structure along selected high-symmetry lines within the first Brillouin zone is shown in Fig. 1. It can be clearly seen that there is no gap at the Fermi level (E_f). The valence and conduction bands overlap greatly and there are considerable bands across the E_f, which is analogous to the major members of MAX phases [1]. As a result, $Ti_5Al_2C_3$ is expected to exhibit thermal and electrical conductivity as good as that of metal. Moreover, an important feature of the band structure is the strong anisotropy with less c-axis energy dispersion. This can be seen from the reduced dispersion along the short H-K and M-L directions. Therefore, the conductivity for single-crystal $Ti_5Al_2C_3$ is also supposed to be anisotropic.

In order to understand the bonding in $Ti_5Al_2C_3$, the total density of states (TDOS) and partial density of states (PDOS) at equilibrium states are calculated, the results of which are shown in Fig. 2. It can be seen that Ti 3d state dominates with less contribution of Al 3p state above the E_f. The TDOS at E_f is 10.6 states/eV unit cell, suggesting that $Ti_5Al_2C_3$ is conductive. The TDOS at the E_f is contributed mainly by the Ti 3d state and secondarily by the Al 3p state. As a result, Ti 3d dominates the conductivity of $Ti_5Al_2C_3$. The C does not contribute to the DOS at the E_f and therefore is not involved in the conduction properties. The energy bands from -1.8 eV to 0 eV are dominated by the hybridized Ti 3d, Ti 3p and Al 3p states. Therefore, $Ti_5Al_2C_3$ appears to have a metallic nature, resembling many of the MAX phases [1]. The lower energy bands in the range of -6.2 eV to -1.8 eV are mainly composed of the Ti 3d, Ti 3p, Al 3p and C 2p hybridized states. This implies $Ti_5Al_2C_3$ could also exhibit a covalent nature. It is interesting to note there are quite a few peaks in the Al 3s and 3p states from -7.2 eV to -2.5 eV, indicating there is *sp* hybridization in Al, i.e. the close-packed layer of Al atoms is bonded as a result of *sp* hybridization. This result is similar to the previous reports on Ti_2AlC and Ti_3AlC_2. The lowest energy bands from -12.1 eV to -8.9 eV originate mainly from the hybridized states of Ti 3d, Ti 3p and C 2p. Clearly, the hybridized Ti and C states are located at a lower energy range compared with Ti-Al hybridization. These results indicate that the Ti-C bonding is stronger than the Ti-Al bonding. These results are similar to those of the conventional MAX phases that typically have exceptionally strong M-X bonds and relatively weak M-A bonds [1,50].

Table 2: The calculated second-order elastic constants C_{ij} (GPa), bulk modulus B (GPa), shear modulus G (GPa), Young's modulus E (GPa) and Poisson's ratio μ of $Ti_5Al_2C_3$ and related phases.

Compound	C_{11}	C_{12}	C_{13}	C_{14}	C_{33}	C_{44}	B	G	E	μ
$Ti_5Al_2C_3$	332	67	62	-0.5	279	119	147	124	290	0.17
Ti_3AlC_2 [4]	368	81	76	0	313	143	168	135	320	0.18
Ti_2AlC [47]	321	76	100	0	318	144	164	127	305	0.19

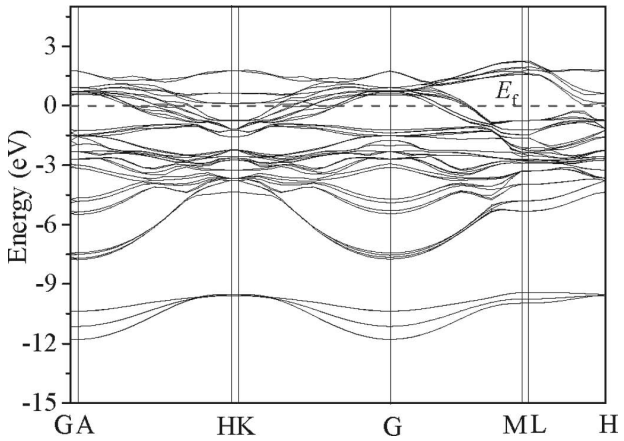

Fig. 1: Calculated band structure along the high symmetry direction in the first Brillouin zone of $Ti_5Al_2C_3$.

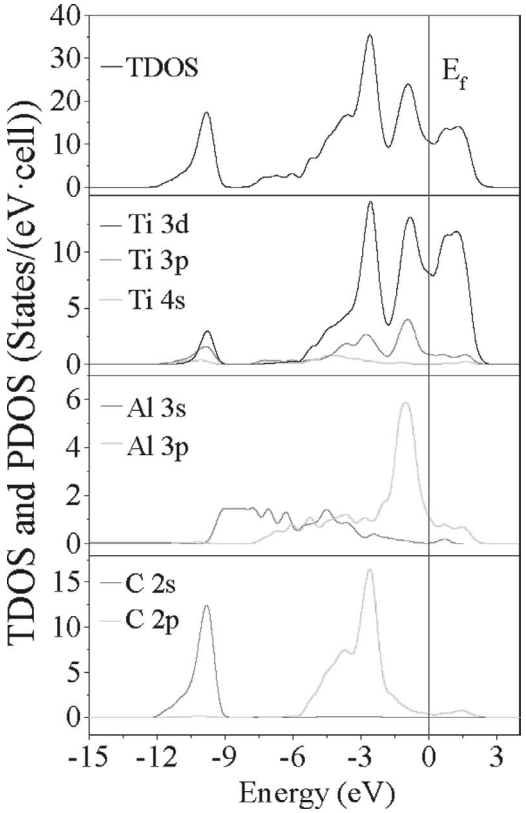

Fig. 2: The calculated total and partial density of states (DOS) for $Ti_5Al_2C_3$. The Fermi energy is set to 0 eV.

IV. Conclusions

In summary, we have studied the structure, elastic and electronic properties of $Ti_5Al_2C_3$ using the first-principles method. The calculated lattice constant and internal coordinates are consistent with the experimental values. The bulk modulus, shear modulus, Young's modulus, Poisson's ratio, theoretical density and Debye temperature of $Ti_5Al_2C_3$ are calculated to be 147 GPa, 124 GPa, 290 GPa, 0.17, 4.12 g/cm^3 and 759 K, respectively. The cohesive energy and Born criteria reveal that $Ti_5Al_2C_3$ is stable. The band structure and DOS show that $Ti_5Al_2C_3$ is conductive. At the E_f, the energy band is originated mainly from the Ti 3d state and secondarily from the Al 3p state. Ti-Al hybridizations are located below the E_f and are weaker than the Ti-C bonds, which are in deeper energy. The authors hope that these theoretical predictions will inspire experimental investigation of $Ti_5Al_2C_3$.

Acknowledgements

This work was financially supported by the project funded by China Postdoctoral Science Foundation (2015M571865), the Preferred Fund of Postdoctoral Scientific Research Project of Zhejiang Province, the Scientific Research Fund of Zhejiang Provincial Education Department (Y201120994) and the National Science Foundation of China (11375079).

References

1. Barsoum, M.W.: The $M_{N+1}AX_N$ phases: A new class of solids; thermodynamically stable nanolaminates, *Prog. Solid State Chem.*, **28**, [1–4], 201–281, (2000).
2. Eklund, P., Beckers, M., Jansson, U., Hogberg, H., Hultman, L.: The $M_{n+1}AX_n$ phases: materials science and thin-film processing, *Thin Solid Films*, **518**, [8], 1851–1878, (2010).
3. Qian, X.K., He, X.D., Li, Y.B., Sun, Y., Li, H., Xu, D.L.: Cyclic oxidation of Ti_3AlC_2 at 1000–1300 °C in air, *Corros. Sci.*, **53**, [1], 290–295, (2011).
4. He, X.D., Bai, Y.L., Zhu, C.C., Sun, Y., Li, M.W., Barsoum, M.W.: General trends in the structural, electronic and elastic properties of the M_3AlC_2 phases (M = transition metal): A first-principle study, *Comput. Mater. Sci.*, **49**, [3], 691–698, (2010).
5. Lin, Z.J., Zhuo, M.J., Zhou, Y.C., Li, M.S., Wang, J.Y.: Atomic scale characterization of layered ternary Cr_2AlC ceramic, *J. Appl. Phys.*, **99**, [7], 076109, (2006).
6. Wang, X.H., Li, F.Z., Chen, J.X., Zhou, Y.C.: Insights into high temperature oxidation of Al_2O_3-forming Ti_3AlC_2, *Corros. Sci.*, **58**, 95–103, (2012).
7. Wang, J.Y., Wang, J.M., Zhou, Y.C., Lin, Z.J., Hu, C.F.: *Ab initio* study of polymorphism in layered ternary carbide M_4AlC_3 (M = V, nb and Ta), *Scripta. Mater.*, **58**, [12], 1043–1046, (2008).
8. Qian, X.K., Li, Y.B., He, X.D., Fan, H.H., Yun, S.N.: First-principle study of structural and electronic properties of ternary layered Ta_2AlC, *J. Phys. Chem. Solids*, **72**, [8], 954–956, (2011).
9. Bai, Y.L., He, X.D., Wang, R.G., Sun, Y., Zhu, C.C., Wang, S., Chen, G.Q.: High temperature physical and mechanical properties of large-scale Ti_2AlC bulk synthesized by self-propagating high temperature combustion synthesis with pseudo hot isostatic pressing, *J. Eur. Ceram. Soc.*, **33**, [13–14], 2435–2445, (2013).
10. Qian, X.K., Li, Y.B., He, X.D., Chen, Y.X., Yu, S.N.: Electrical and thermal properties of Ti_3AlC_2 at high temperature, *J. Ceram. Sci. Tech.* **2**, [3], 155–158, (2011).
11. Wang, X.H., Zhou, Y.C.: Oxidation behavior of Ti_3AlC_2 at 1000–1400 °C in air, *Corros. Sci.*, **45**, [5], 891–907, (2003).
12. Qian, X.K., He, X.D., Li, Y.B., Sun, Y., Zhu, C.C.: Improving the cyclic-oxidation resistance of Ti_3AlC_2 at 550 °C and 650 °C by preoxidation at 1100 °C, *Int. J. Appl. Ceram. Tech.*, **7**, [6], 760–765, (2010).
13. Qian, X.K., Li, Y.B., Sun, Y., He, X.D., Zhu, C.C.: Cyclic oxidation behavior of TiC/Ti_3AlC_2 composites at 550–950 °C in air, *J. Alloy. Compd.*, **491**, [1–2], 386–390, (2010).
14. Gupta, S., Hoffman, E.N., Barsoum, M.W.: Synthesis and oxidation of Ti_2InC, Zr_2InC, $(Ti_{0.5},Zr_{0.5})_2InC$ and $(Ti_{0.5},Hf_{0.5})_2InC$ in air, *J. Alloy. Compd.*, **426**, [1–2], 168–175, (2006).
15. Lin, Z.J., Li, M.S., Wang, J.Y., Zhou, Y.C.: High-temperature oxidation and hot corrosion of Cr_2AlC, *Acta Mater.*, **55**, [18], 6182–6191, (2007).

16. Jovic, V.D., Jovic, B.M., Gupta, S., El-Raghy, T., Barsoum, M.W.: Corrosion behavior of select MAX phases in NaOH, HCl and H_2SO_4, *Corros. Sci.*, **48**, [12], 4274 – 4282, (2006).
17. Barsoum, M.W., Zhen, T., Kalidindi, S.R., Radovic, M., Murugaiah, A.: Fully reversible, dislocation-based compressive deformation of Ti_3SiC_2 to 1 GPa, *Nat. Mater.*, **2**, [2], 107 – 111, (2003).
18. He, X.D., Bai, Y.L., Li, Y.B., Zhu, C.C., Kong, X.H.: *In situ* synthesis and mechanical properties of bulk Ti_3SiC_2/TiC composites by SHS/PHIP, *Mater. Sci. Eng. A*, **527**, [18 – 19], 4554 – 4559, (2010).
19. Patel, M.K., Tallman, D.J., Valdez, J.A., Aguiar, J., Anderoglu, O., Tang, M., Griggs, J., Fu, E., Wang, Y.,Barsoum, M.W.: Effect of helium irradiation on Ti_3AlC_2 at 500 °C, *Scripta Mater.*, 771 – 774, (2014).
20. Song, G.M., Li, S.B., Zhao, C.X., Sloof, W.G., van der Zwaag, S., Pei, Y.T., de Hosson, J.T.M.: Ultra-high temperature ablation behavior of Ti_2AlC ceramics under an oxyacetylene flame, *J. Eur. Ceram. Soc.*, **31**, [5], 855 – 862, (2011).
21. Huang, Z., Zhai, H., Li, M., Liu, X., Zhou, Y.: Friction behaviors and effects on current-carrying wear characteristics of bulk Ti_3AlC_2, *Tribol. Trans.*, **57**, [2], 300 – 307, (2014).
22. Xu, J., Yan, H., Gu, D.: Friction and wear behavior of polytetrafluoroethene composites filled with Ti_3SiC_2, *Mater. Design*, **61**, 270 – 274, (2014).
23. Palmquist, J.P., Li, S., Persson, P.O.A., Emmerlich, J., Wilhelmsson, O., Hogberg, H., Katsnelson, M.I., Johansson, B., Ahuja, R., Eriksson, O., Hultman, L., Jansson, U.: $M_{n+1}AX_n$ phases in the Ti-Si-C system studied by thin-film synthesis and *ab initio* calculations, *Phys. Rev. B*, **70**, [16], 165401, (2004).
24. Hogberg, H., Eklund, P., Emmerlich, J., Birch, J., Hultman, L.: Epitaxial Ti_2GeC, Ti_3GeC_2, and Ti_4GeC_3 MAX-phase thin films grown by magnetron sputtering, *J. Mater. Res.*, **20**, [4], 779 – 782, (2005).
25. Lane, N.J., Naguib, M., Lu, J., Hultman, L., Barsoum, M.W.: Structure of a new bulk $Ti_5Al_2C_3$ MAX phase produced by the topotactic transformation of Ti_2AlC, *J. Eur. Ceram. Soc.*, **32**, [12], 3485 – 3491, (2012).
26. Zhou, Y.C., Meng, F.L., Zhang, J.: New MAX-phase compounds in the V-Cr-Al-C system, *J. Am. Ceram. Soc.*, **91**, [4], 1357 – 1360, (2008).
27. Zhang, H., Wang, X.H., Ma, Y.H., Sun, L.C., Zheng, L.Y., and Zhou, Y.C.: Cystal structure determination of nanolaminated $Ti_5Al_2C_3$ by combined techniques of XRPD, TEM and *ab initio* calculations, *J. Adv. Ceram.*, **1**, [4], 268 – 273, (2012).
28. Hu, C.F., Zhang, H.B., Li, F.Z., Huang, Q., Bao, Y.W.: New phases' discovery in MAX phase, *Int. J. Refract. Met. H.*, **36**, 300 – 312, (2013).
29. Lin, Z.J., Zhuo, M.J., Zhou, Y.C., Li, M.S., Wang, J.Y.: Microstructural characterization of layered ternary Ti_2AlC, *Acta Mater.*, **54**, [4], 1009 – 1015, (2006).
30. Wilhelmsson, O., Palmquist, J.P., Lewin, E., Emmerlich, J., Eklund, P., Persson, P.O.A., Hogberg, H., Li, S., Ahuja, R., Eriksson, O., Hultman, L., Jansson, U.: Deposition and characterization of ternary thin films within the Ti-Al-C system by DC magnetron sputtering, *J. Cryst. Growth*, **291**, [1], 290 – 300, (2006).
31. Wang, X.H., Zhang, H., Zheng, L.Y., Ma, Y.H., Lu, X.P., Sun, Y.J., Zhou, Y.C.: $Ti_5Al_2C_3$: A new ternary carbide belonging to MAX phases in the Ti-Al-C system, *J. Am. Ceram. Soc.*, **95**, [5], 1508 – 1510, (2012).
32. Lane, N.J., Naguib, M., Lu, J., Eklund, P., Hultman, L., Barsoum, M.W.: Comment on "$Ti_5Al_2C_3$: A new ternary carbide belonging to MAX phases in the ti-al-C system", *J. Am. Ceram. Soc.*, **95**, [10], 3352 – 3354, (2012).
33. Anisimov, V.I., Aryasetiawan, F., Lichtenstein, A.I.: First-principles calculations of the electronic structure and spectra of strongly correlated systems: the LDA+U method, *J. Phys. Condes. Mat.*, **9**, [4], 767 – 808, (1997).
34. Jiao, Z.Y., Ma, S.H., Huang, X.F.: A first-principles study on the structural, mechanical, electronic and optical properties of the $Cr_2(Al_xGe_{1-x})C$ alloys, *J. Alloy. Compd.*, **583**, 607 – 613, (2014).
35. Xu, Y.G., Ou, X.D., Rong, X.M.: Vacancy trapping behaviors of hydrogen in Ti_3SiC_2: A first-principles study, *Mater. Lett.*, **116**, 322 – 327, (2014).
36. Qian, X.K., Wang, N., Li, Y.X., Zhou, Y., Wu, H.X., Li, Y.B., He, X.D.: First-principle studies of properties of ternary layered M_2PbC (M = Ti, Zr and Hf), *Comput. Mater. Sci.*, **65**, 377 – 382, (2012).
37. Bai, Y.L., He, X.D., Wang, R.G., Zhu, C.C.: An *ab initio* study on compressibility of Al-containing MAX-phase carbides, *J. Appl. Phys.*, **114**, [17], 173709, (2013).
38. Zhao, S.J., Xue, J.M., Wang, Y.G., Huang, Q.: First-principles investigation of the intrinsic defects in Ti_3SiC_2, *J. Phys. Chem. Solids*, **75**, [3], 384 – 390, (2014).
39. Wu, H.Y., Qian, X.K., Zhu, H.P., Lei, J., He, X.D.: First-principles study of the structural, electronic and elastic properties of ternary Zr_2AN (*A* = Ga, In and Ti), *Comput. Mater. Sci.*, **84**, 103 – 107, (2014).
40. Li, C.L., Wang, Z.Q., Wang, C.Y.: Phase stability, mechanical properties and electronic structure of hexagonal and trigonal $Ti_5Al_2C_3$: An *ab initio* study, *Intermetallics*, **33**, 105 – 112, (2013).
41. Segall, M.D., Lindan, P.J.D., Probert, M.J., Pickard, C.J., Hasnip, P.J., Clark, S.J., Payne, M.C.: First-principles simulation: ideas, illustrations and the CASTEP code, *J. Phys. Condens. Mat.*, **14**, [11], 2717 – 2744, (2002).
42. Monkhorst, H.J., Pack, J.D.: Special points for Brillouin-zone integrations, *Phys. Rev. B*, **135**, 188 – 5192, (1976).
43. Vanderbilt, D.: Soft self-consistent pseudopotentials in a generalized eigenvalue formalism, *Phys. Rev. B*, **41**, [11], 7892 – 7895, (1990).
44. Perdew, J.P., Burke, K., Ernzerhof, M.: Generalized gradient approximation made simple, *Phys. Rev. Lett.*, **77**, [18], 3865 – 3868, (1996).
45. Pfrommer, B.G., Cote, M., Louie, S.G., Cohen, M.L.: Relaxation of crystals with the quasi-newton method, *J. Comput. Phys.*, **131**, [1], 133 – 140, (1997).
46. Hill, R.: The elastic behaviour of a crystalline aggregate, *Proc. Phys. Soc. London*, **65**, [389] 349 – 355, (1952).
47. Gan, Y.P., Qian, X.K., He, X.D., Chen, Y.X., Yun, S.N., Zhou, Y.: Structural, elastic and electronic properties of a new ternary-layered Ti_2SiN, *Physica B*, **406**, [20], 3847 – 3850, (2011).
48. Sun, Z.M., Li, S., Ahuja, R., Schneider, J.M.: Calculated elastic properties of M_2AlC (M = Ti, V, Cr, Nb and Ta), *Solid State Commun.*, **129**, [9], 589 – 592, (2004).
49. Bai, Y.L., He, X.D., Sun, Y., Zhu, C.C., Li, M.W., Shi, L.P.: Chemical bonding and elastic properties of Ti_3AC_2 phases (A = Si, Ge, and Sn): A first-principle study, *Solid State Sci.*, **12**, [7], 1220 – 1225, (2010).
50. Zhu, H.P., Qian, X.K., Wu, H.Y., Lei, J., Song, Y.C., He, X.D., Zhou, Y.: Cyclic oxidation of ternary layered Ti_2AlC at 600 – 1000 °C in air, *Int. J. Appl. Ceram. Tech.*, **12**, [2], 403 – 410, (2015).